# STRUCTURAL RELATIONSHIPS IN THE PSEUDO-BINARY SYSTEM

# $ZrFe_2$-$ZrCr_2$

MASS. INST. OF TECHNOLOGY
DEC 1959
LIBRARY

by

Simon Charles Moss

SUBMITTED IN PARTIAL FULFILLMENT OF THE

REQUIREMENTS OF THE DEGREE OF

MASTER OF SCIENCE

at the

MASSACHUSETTS INSTITUTE OF TECHNOLOGY

August 1959

Signature of author_____

Signature of Thesis Supervisor_____

Signature of Chairman of
Departmental Committee
on Graduate Students_____

# STRUCTURAL RELATIONSHIPS IN THE PSEUDO-BINARY SYSTEM $ZrFe_2$-$ZrCr_2$

by

Simon Charles Moss

Submitted to the Department of Metallurgy on August 24, 1959, in Partial Fulfillment of the Requirements for the Degree of Master of Science

## ABSTRACT

Structural relationships were studied among ternary Laves phases in the system $ZrFe_2$-$ZrCr_2$. Among the phenomena observed was the allotropy in $ZrCr_2$, which was shown to exhibit a high temperature modification of the hexagonal C14 structure type close to the melting point and a low temperature modification of the C15 cubic type. In connection with the latter observation was the fact that at 890°C Fe was soluble in C15 $ZrCr_2$ up to ~ 8 percent followed by a narrow two phase region and then a single phase region extending from ~ 20 percent Fe to ~ 80 percent Fe of the C14 structure type. After a very narrow two phase region, the C15 cubic structure appeared again at 90 percent Fe and at $ZrFe_2$. At the Fe rich end the cubic structure appeared to be stable at 890°C, 1000°C and 1400°C to the same degree of solubility. At the Cr rich end the C15 structure seemed to decrease in solubility with increasing temperature.

On the basis of these observations a proposed pseudo-binary phase diagram was drawn enclosing the C15 $ZrCr_2$ with a gamma loop and allowing the C14 high temperature phase to extend its solubility over to ~ 80 per cent Fe. A peritectic reaction was employed to account for the cubic to hexagonal transformation at the iron rich end.

From X-ray data, the lattice constant of both the cubic and hexagonal phases were solved and size effects were plotted against composition. It was seen that A-A (Zr-Zr) atom distances were most distorted at the Cr rich end and that B-B distances (Fe,Cr-Fe,Cr) were distorted abruptly due to the transformation near the Fe rich end. The transformations observed were partially explained on the basis of these size factors.

Thesis Supervisor: R. F. Ogilvie, Assistant Professor of Metallurgy

# Table of Contents

# List of Illustrations

## List of Tables

## Acknowledgements

The author would like to express his thanks to Professor Robert Ogilvie for the suggestion of the thesis subject and for advice in the course of this work and to Professor John T. Norton for his helpful discussions. Thanks are also due to Dr. Erwin Parthé for the many insights into the problem that he provided and to Dr. Roy Kaplow for his assistance in writing a program for the IBM 704 computer.

For experimental help the author would like to thank Mr. Norman Peterson for the use of some of his equipment and the members of the Ceramics Department for the use of their high temperature furnaces.

To Mrs. Dorothy Bowe go thanks for the initial preparation of the manuscript, and to my wife, Peggy, for the final typing.

# I. Introduction

The system $ZrFe_2$-$ZrCr_2$ is representative of a number of ternary sections between two binary intermetallic compounds of the formula $AB_2$ known as Laves phases. The study of such a pseudo-binary section and the solubility limits of the binary phases should give much information about the structural behavior and nature of these phases.

Much is known already about the three Laves phases and some of the size factors and electronic considerations that contribute to their stability and make them some of the most frequently observed structures in metal systems. Below are listed these three phases, their space groups, cell types, and other structural characteristics along with the original references.

a. $MgCu_2$ - cubic C15 type, $O_h^7$ - Fd3m
   24 atoms per unit cell, a = 7.03kx, ref. Friauf[1]

b. $MgZn_2$ - hexagonal C14 type, $D_{6h}^4$ - $P6_3/mmc$
   12 atoms per unit cell, a = 5.15 kx
   c/a = 1.65, ref. Friauf[2]

c. $MgNi_2$ - hexagonal C36 type, $D_{6h}^4$ - $P6_3/mmc$
   24 atoms per unit cell, a = 4.81 kx
   c/a = 3.28, ref. Laves and Witte[3]

In Figure 1 may be seen the basic structural similarity among the Laves phases. $MgCu_2$ has a stacking of ABC/ABC when

viewed hexagonally along a $\langle 111 \rangle$ direction of the unit cube. $MgZn_2$ shows stacking of the AB/AB while $MgNi_2$ is intermediate between the latter two having a stacking ABAC/ABAC. Laves, in his excellent discussion in the book "Theory of Alloy Phases"[4] has shown that these three compounds of the $MgX_2$ type may be considered "homeotect"; that is, they all have the same construction formula or nearest neighbor coordination and distance. Thus the Mg atoms always have a four fold lattice coordination with respect to each other but are surrounded by 12 X atoms, while the X atoms exhibit six fold lattice coordination with each other and with their nearest Mg neighbors. This purely geometrical relationship gives rise to the condition that the theoretical ratio of atom sizes in any of the three Laves phases, $AB_2$, is $D_A/D_B = \sqrt{3}/\sqrt{2} = 1.255$. The geometry by similar reasoning restricts the value of the hexagonal axial ratio for each case. These axial ratios for the three types C14, C15, and C36 are in the relationship 2:3:4, respectively.

The theoretical ratio of atom sizes, based upon either the distance as measured in the pure metal or upon this distance corrected to twelve fold coordination, in Laves phases allows both A-A and B-B contacts but denies A-B contact. The individual compounds may thus be considered as interpenetrating lattices of A atoms and B atoms. Furthermore any deviation from the theoretical value of $D_A/D_B = 1.225$ will produce expan-

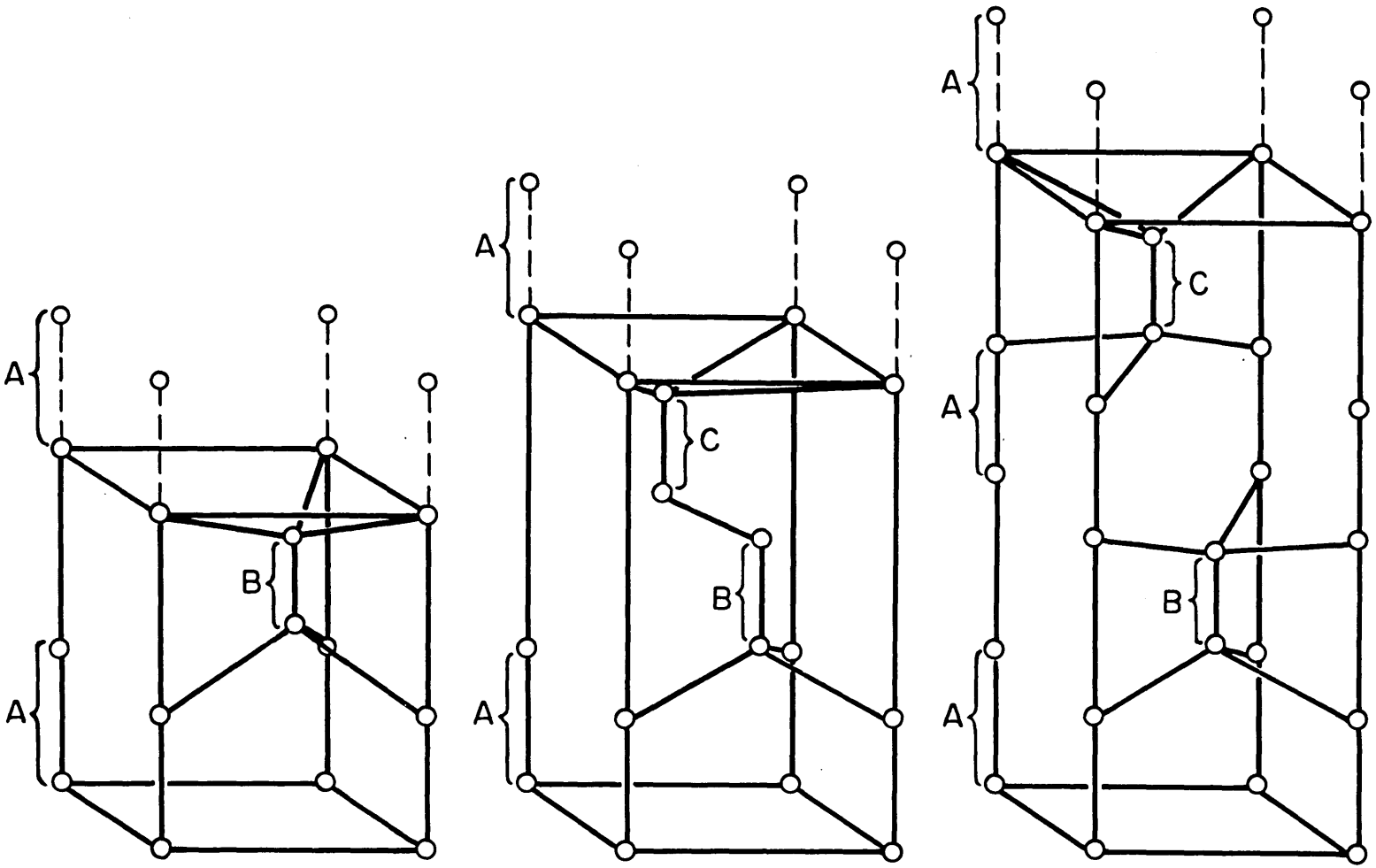


C14 – $MgZn_2$ C15 – $MgCu_2$ C36 – $MgNi_2$

FIGURE 1 THE ARRANGEMENT OF THE LARGE A ATOMS IN THE THREE LAVES PHASES

sion in one set of distances and contraction in the other. Except in isolated instances, the Laves phase cannot sustain large deviations from the ideal size ratio and most of the compounds known of these types tend to cluster in a range of $D_A/D_B$ from about 1.15 to 1.35.

The very high degree of space filling and associated stability of bonding account to a large extent for the many known Laves type compounds. Massalski[5] has indicated that for Laves phases the size effect is most probably the sine qua non while other factors such as electron configuration or concentration probably play the leading role in the selection of the specific modification. This reasoning is due in a large part to the work of Klee and Witte[6] who calculated, by means of magnetic measurements, the electron concentration of the Brillouin zones for the $MgCu_2$, $MgNi_2$ and $MgZn_2$ types in the quasi-binary system $MgCu_2$-$MgZn_2$. They thus effectively established electron concentration ranges of stability for each of the three modifications. Also the much earlier work of Laves and Witte[7] established more empirically the ranges of valence electron concentration for the C15, C36 and C14 structure types. Elliott[8] recently has employed these limits of electron concetration to calculate the valencies of transition elements. He worked with quasi-binary sections of ternary Laves phase extending between sets of two known binary transi-

tional element Laves phases. To the solubility limits of each type (C14, C15) in these ternary sections he assigned the electron per atom ratio as given by Laves and Witte[7] and from pairs of simultaneous equations calculated transition element valencies. The general validity of this method and its applicability to the present problem will be discussed later.

That the atomic size ratio $D_A/D_B$ might play a more sophisticated role in the determination of Laves phases was suggested in a paper by Berry and Raynor[9]. They proposed that in addition to predicting Laves phases in a general sense the size ratio, when analysed more completely, seems to indicate which modification will be stable. Due to the infrequent occurrence of the C36 ($MgNi_2$) type their analysis was confined mainly to the C14 and C15 types. They showed that clustered about the ideal ratio of 1.225 lie most of the known C14 compounds, while at larger deviations from that value, correllated with greater distortions in both A-A and B-B distances, lie most of the C15 types. They indicated further that even at the ideal ratio the distortions, expressed as percentages of the sizes in the pure metal, did not vanish, thus implying A-B interaction based most probably upon electronic effects. They restricted their plots of $D_A/D_B$ versus percent distortion in the case of Zr as the A element to a series of separate curves for each subgroup of the transition

metals. In this manner the distortion introduced by Fe, Ru and Os lay on one set of curves while those of Mn and Re lay on another. This selection of data presentation again suggests that electronic effects must be considered.

To the general atmosphere of complexity must be added the additional fact that some Laves phases, notably $TaCr_2$, $TiCr_2$ and $ZrCr_2$, show structural allotropy favoring C14 at one temperature and C15 at another. In the case of $TaCr_2$ and $TiCr_2$ the high temperature phase is generally agreed to be of the $MgZn_2$, C14 type. In the case of $ZrCr_2$, first reported by Wallbaum[10] as C14, there has been some controversy. The U. S. Bureau of Mines[11] reported the compound as cubic C15 and the controversy was seemingly resolved when Rostoker[12] reported an allotropic change from the low temperature C14 to the high temperature C15 type occurring at between 900° and 1000°C. Jordan and Duwez[13] disagreed with Rostoker, reporting the allotropy to be in the opposite direction with C14 $ZrCr_2$ as the high temperature modification existing in a region quite near the melting point and C15 as the stable low temperature structure. They explained the existing confusion on kinetic grounds stating that the apparent transformation near 1000°C from C14 (quenched in the arc-melted button) to C15 was really due to an increase in the kinetic rate of the transformation which, were it not denied by rate considerations,

would have occurred at the lower temperatures of 600°C, 700°C and 800°C. They supported this conclusion by taking a sample of pure C15 and heating to near the melting point where they then noticed a partial re-transformation to C14. Elliott[14] confirmed Rostoker's observation and the present work for reasons to be discussed must agree with the conclusions of Jordan and Duwez.

As to the structure of $ZrFe_2$, the other binary component of the system here studied, there is no disagreement with the original work of Wallbaum[15] who reported it to be isomorphous with the cubic C15 type. The compound can accommodate up to about six additional percent of Fe and still retain its structure[13, 15].

# II. Experimental Procedure

## A. Alloy Preparation

For the purpose of examining the structural relationships in the system $ZrFe_2$-$ZrCr_2$, eleven alloys were prepared at each ten atomic percent of Cr from the pure $ZrFe_2$ to the pure $ZrCr_2$. The fifty gram buttons were arc melted under an inert atmosphere in a water cooled copper crucible and were turned and re-melted several times to provide good homogeneity. After the final melting the surfaces showed no signs of oxidation. A chemical analysis was made of each, the results of which are reported in Table I. It may be seen that in many cases the Zr percent reads a little low. This may be due to the accuracy of the analysis or to improper weighing of the constituent elements prior to melting. The latter would seem correct in view of the vaporization which occurred during the high temperature heat treatments and which was mainly attributable, by X-ray fluorescent analysis of the deposits, to a slight excess of chromium in the alloys. Since the solubility limits of $ZrCr_2$ form quite a narrow range any excess Cr allows the formation of a two phase alloy of $Zr(Fe, Cr)_2$ and nearly pure chromium. It is the chromium in this latter phase which having so high a vapor pressure, appeared as a deposit during treatment. It is not felt that the stoichiometry of the intermetallic phases, either binary or ternary, was altered due to the

TABLE I

Chemical Analysis of the Alloys Prepared by Arc Melting

Compared with Calculated Percentages in Weight %

| Sample | Chemical Analysis | | | | Calculated Values | | |
|---|---|---|---|---|---|---|---|
| | % Zr | % Fe | % Cr | %O | % Zr | % Fe | % Cr |
| $ZrFe_2$ | 43.6 | 55.4 | -- | 0.093 | 44.98 | 55.02 | -- |
| $ZrFe_{1.8}Cr_{.2}$ | 44.3 | 49.8 | 5.01 | 0.099 | 45.12 | 49.74 | 5.14 |
| $ZrFe_{1.6}Cr_{.4}$ | 44.5 | 44.8 | 10.25 | 0.091 | 45.28 | 44.38 | 10.34 |
| $ZrFe_{1.4}Cr_{.6}$ | 44.0 | ? | 15.7 | 0.086 | 45.50 | 38.94 | 15.56 |
| $ZrFe_{1.2}Cr_{.8}$ | 45.0 | 33.9 | 20.9 | 0.093 | 45.64 | 33.54 | 20.82 |
| ZrFeCr | 45.1 | 28.9 | 26.5 | 0.090 | 45.82 | 28.04 | 26.14 |
| $ZrFe_{.8}Cr_{1.2}$ | 46.0 | 22.8 | 31.3 | 0.098 | 46.00 | 22.52 | 31.48 |
| $ZrFe_{.6}Cr_{1.4}$ | 45.7 | 17.2 | 37.1 | 0.082 | 46.18 | 16.96 | 36.86 |
| $ZrFe_{.4}Cr_{1.6}$ | 46.3 | 11.5 | 42.5 | 0.077 | 46.36 | 11.34 | 42.30 |
| $ZrFe_{.2}Cr_{1.8}$ | 46.0 | 6.0 | 47.9 | 0.080 | 46.52 | 5.72 | 47.76 |
| $ZrCr_2$ | 46.2 | -- | 53.2 | 0.074 | 46.72 | -- | 53.28 |

process of vaporization.

B. X-ray Measurements

Prior to any heat treating the arc melted buttons were broken in a small mortar and a few of the smaller pieces were taken from each at random and further crushed and sifted to -325 mesh. Diffraction patterns were then made using a Debye Scherrer camera of 57.3 mm in diameter with Straumanis mounting. The powder, collected on coated paper, was then applied to a finely drawn glass fiber coated with a dilute misture of vaseline and petroleum ether by rolling the fiber, mounted in the specimen holder of the camera, over the powder. $CuK_{\alpha}$ radiation (1.54178Å) was used at a K.V. of 35 and at 10 m.a. for an average exposure time of two and one-half hours.

These preliminary patterns were taken, not for any precise measurement of lattice constant, but rather to establish generally which of the modifications of the Laves phases, if any, formed upon direct quench from the melt. It was suspected, of course, that some coring would occur in buttons melted in the above described fashion as well as some variation in homogeneity. However in the case of the binary components, $ZrFe_2$ and $ZrCr_2$ which melt congruently, a very good idea of any high temperature structure can be obtained in this manner, unless such a structure cannot be retained at lower temperatures.

If the latter should be true then a transformation to a second structure should not be observed as the temperature is raised. The only objection to this argument requires a very fortuitous arrangement of temperature gradients in the cooling button (within the crucible) that would essentially heat treat the alloy and stabilize the low temperature configuration, transforming to it from the high temperature one.

C. Heat Treatments

From references to past studies[13, 14] appropriate heat treatments were outlined for the entire series. One set of alloys was treated at 1400°C for one hour in separate crucibles of boron nitride in a vacuum induction furnace that maintained a constant pressure of $10^{-4}$ mm Hg. A second and third set were individually wrapped in Ta foil of .001" thickness and sealed into evacuated clear quartz tubes at a pressure of $5 \times 10^{-6}$ mm Hg. The tubes of the second set (six specimens in one tube, five in the other) were then placed in a 30 inch long horizontal Kanthal wound furnace at 1000°C for three days. The temperature gradient was such to maintain temperature over an 8 inch length to within $\pm 3^{o}$.[16] After treatment the tubes were air cooled and then broken open. The third set were placed in similar furnaces at 890°C for 30 days and cooled in the same manner.

In addition to these runs, selected treatments were made

at 800°C and 890°C. At the lower temperature two samples, $ZrFe_2$ and $ZrCr_2$ both as melted, were treated for four days to improve uniformity of composition and relieve any stresses. At 890°C two samples of $ZrCr_2$ were treated for 15 days, one of which was in the as-melted condition. The other sample had been previously treated at 1400°C for one hour and was known to be of the C15 modification while the first was of the C14 type. See Table II for a summary of these procedures.

The alloys thus treated were then broken and small portions from the centers of each were crushed to -325 mesh powder. In all cases they proved quite brittle and crushed easily. X-ray film patterns were made from these powders as outlined above.

TABLE II

A Summary of the Heat Treatments Performed

| Samples | Containers | Furnace | Temp. | Time |
|---|---|---|---|---|
| Eleven alloys $ZrFe_2$-$ZrCr_2$ | Individual BN Crucibles | Vacuum Induction | 1400°C | 1 hour |
| Eleven alloys $ZrFe_2$-$ZrCr_2$ per temp. | Ind. wrapped in TA foil (.001") sealed in clear quartz tubes at 5 x $10^{-6}$ mm Hg. | Horizontal Kanthal Wound | 1000°C | 3 days |
| | | | 890°C | 30 days |
| $ZrCr_2$ (as melted) and $ZrCr_2$ (previously treated at 1400°C - 1 hour) | As above | As above | 890°C | 15 days |

## III. Calculations and Results

### A. Indexing the Diffraction Pattern

Because of the structural similarity of the three Laves phases C14, C15 and C36, one would expect their diffraction patterns to bear some resemblance. Indeed the three have much in common. For example, if it is remembered that they all may be represented as hexagonal with equal $a_o$ parameters and with the $c_o$ parameters in the ratio of 2:3:4, all reflections of the type h k o fall at the same angular position, extinction conditions permitting, and conversely, at the same angular position fall reflections in the order 0 0 $\ell$, 0 0 3/2 $\ell$, 0 0 2 $\ell$ where $\ell = 2n$. Elliott[8] has tabulated these common reflections which are given in Table III.

In the case of the cubic C15 structure, the space group ($O_h^7$ - F d3m) shows it to be basically a face-centered lattice with additional symmetry elements giving rise to extra extinctions. The indexing of this pattern is a simple matter and intensity relationships need not be referred to.

For the C14 and C36 structures accurate indexing becomes more of a problem and reliance upon such a technique as the Hull-Davey chart is of little use. The C14 and C36 types are such that all C14 reflections may be read as C36 with double the $\ell$ index whereas there are some extra C36 lines that do not occur in the C14 pattern. An example of this latter type is

TABLE III

Equivalent Indices of Common

Reflections of Laves Type Phases

| $MgCu_2$ | $MgZn_2$ | $MgNi_2$ |
|---|---|---|
| 220 | 11.0 | 11.0 |
| 311 | 11.2 | 11.4 |
| 222 | 00.4 | 00.8 |
| 422 | 30.0 | 30.0 |
| 411/333 | 30.2 | 30.4 |
| 440 | 22.0 | 22.0 |
| 620 | 10.7 | 10.14 |

the set of reflections h h $l$ where $l$ must be equal to 2n. C14 will show only those reflections where $l$ = 4n for C36 since 4n/2 = 2n, and the extinction condition thus still applies to the C14 structure with one-half the $l$ index of C36.

The most convenient way of properly indexing the diffraction pattern as C14, which in all cases in question it appeared to be, is by calculation of line intensities according to the formula:

$$I \sim |F|^2 \times m \times L.P. \qquad (1)$$

where: F = structure factor

m = planar multiplicity

L.P. = combined Lorenz and polarization factors.

Where any appreciable amount of iron exists in the structure, i.e. $Zr(Fe,Cr)_2$, since $CuK_\alpha$ radiation was used, a Hönl correction should be applied to the atomic scattering factor of iron. However, in this case when the C14 modification of $ZrCr_2$ had been correctly indexed the other alloys whose patterns bore a resemblence to the latter were indexed by visual comparison.

The actual work of intensity calculation can be rather time-consuming, but it was considered necessary as the tabulated values in the report of Jordan and Duwez[13] as well as their indexing of the $ZrCr_2$ patterns, was found to be incomplete, and the discrepancies between their measured and calculated

intensities could not be reconciled on the basis of the explanation given therein.

The calculation of intensities was accelerated greatly through the use of the IBM 704 computer at the M. I. T. Computation Center. The structure factor is usually separated in these calculations into a phase or geometrical factor, depending only upon the discrete values of the atom coordinates and the h, k, $\ell$ values of the separate lattice planes and a scattering factor, $f_n$, which is a continuous function of $\sin \theta/\lambda$ for each component metal. It is in the calculation of the phase factor, A, the general form of which is given under its appropriate space group in the International Tables for X-ray Crystallography, German edition, to which the computer was applied. In Appendix I may be seen the general breakdown of these calculations. The values of $\theta$ for this purpose were obtained from Elliott's calculation of the lattice constants of $ZrCr_2$ [14].

## B. Calculations of the Lattice Constants

Having obtained the intensity values, the observed values of $\sin^2\theta$ were compared with those calculated from Elliott and the measured values of I with the intensities calculated and a preliminary indexing was accomplished. It was noticed that in the high angle range there were many lines of

comparable intensity that lay too close together to be resolved and that others were too weak to observe. From the total set four lines were chosen whose θ values were greater than 50°, and they were solved by a least squares technique for the constants $a_o$ and $c_o$ of $ZrCr_2$. No weighting function for the error was chosen because while the lower angle lines were less accurate, they were more easily measured than the weaker but higher angle lines. In Appendix II is reproduced a sample least squares solution. From the above values of $c_o$ and $a_o$, $\sin^2\theta$ values were re-calculated and a good comparison was found with the measured values. Shown in Table IV is a summary of all of these data on C14 $ZrCr_2$.

For the C15 structure, the lattice constant $a_o$ was solved by extrapolation of the high angle lines to $\theta = 90^o$ against the function of Nelson and Riley[17]. The values of the latter were obtained from Smithell's[18] and all data for the intensity calculations, other than the phase factors, were taken from Cullity[19].

## C. Results

Tables V and VI summarize the total data taken both as to lattice constants and to the structure types. The lattice constants were measured on the 890°C treatments since it is believed that these offered the best combination of homogeneity and purity. However, the samples of $ZrCr_2$ and $ZrFe_{.2}Cr_{1.8}$

TABLE IV

$ZrCr_2$ (C14 Modification) Arc Melted

and Annealed at 800°C for Four Days

| hk·l | $\sin^2\theta$ Calculated (Å) $a_o = 5.093$, $c_o = 8.273$ | $\sin^2\theta$ Observed | Intensity Calculated | Intensity Observed |
|---|---|---|---|---|
| 100 | .0306 | -- | 11 | -- |
| 002 | .0347 | -- | 2 | -- |
| 101 | .0393 | -- | 25 | -- |
| 102 | .0653 | -- | 84 | -- |
| 110 | .0917 | .0916 | 578 | M |
| 103 | .1087 | .1094 | 1000 | MS |
| 200 | .1222 | -- | 16 | -- |
| 112 | .1264 | .1262 | 1164 | S |
| 201 | .1309 | .1309 | 778 | MS |
| 004 | .1389 | .1386 | 128 | MW |
| 202 | .1569 | .1547 | 61 | VW |
| 104 | .1695 | .1701 | 78 | VW |
| 203 | .2003 | -- | 2 | -- |
| 210 | .2139 | -- | 2 | -- |
| 211 | .2226 | -- | 5 | -- |
| 105 | .2477 | .2477 | 140 | VW |
| 212 | .2486 | -- | 23 | -- |
| 204 | .2611 | -- | 4 | -- |

TABLE IV continued

| hk·l | $\sin^2\theta$ Calculated ($a_o$ = 5.093, $c_o$ = 8.273 Å) | $\sin^2\theta$ Observed | Intensity Calculated | Intensity Observed |
|---|---|---|---|---|
| 300 | .2750 | .2761 | 97 | VW |
| 213 | .2920 | .2927 | 376 | W |
| 302 | .3047 | .3111 | 248 | W |
| 006 | .3126 | -- | 55 | -- |
| 205 | .3393 | .3404 | 302 | W |
| 106 | .3432 | -- | 31 | -- |
| 214 | .3528 | -- | 41 | -- |
| 220 | .3666 | .3671 | 261 | MW |
| 310 | .3972 | -- | 1 | -- |
| 222 | .4013 | -- | 3 | -- |
| 116 | .4043 | -- | 3 | -- |
| 311 | .4059 | -- | 2 | -- |
| 215 | .4310 | -- | 58 | -- |
| 312 | .4319 | -- | 9 | -- |
| 206 | .4348 | .4354 | 97 | W |
| 107 | .4560 | .4578 | 27 | VVW |
| 313 | .4753 | .4744 | 174 | W |
| 400 | .4888 | -- | 16 | -- |
| 401 | .4975 | .4953 | 83 | VW |
| 224 | .5055 | .5058 | 90 | VW |

TABLE IV continued

| hk·l | $\sin^2\theta$ Calculated ($a_o$ = 5.093, $c_o$ = 8.273) | $\sin^2\theta$ Observed | Intensity Calculated | Intensity Observed |
|---|---|---|---|---|
| 402 | .5235 | -- | 8 | -- |
| 216 | .5265 | -- | 35 | -- |
| 314 | .5361 | -- | 24 | -- |
| 207 | .5476 | -- | 10 | -- |
| 008 | .5557 | -- | 1 | -- |
| 403 | .5669 | -- | 1 | -- |
| 320 | .5805 | -- | 1 | -- |
| 108 | .5863 | .5915 | 55 | VVW |
| 306 | .5876 | -- | 2 | -- |
| 321 | .5892 | -- | 1 | -- |
| 315 | .6143 | .6154 | 43 | VVW |
| 322 | .6152 | -- | 6 | -- |
| 404 | .6277 | -- | 1 | -- |
| 217 | .6393 | -- | 42 | -- |
| 410 | .6416 | .6449 | 66 | W |
| 118 | .6474 | | 67 | |
| 323 | .6586 | .6590 | 143 | W |
| 412 | .6763 | .6787 | 204 | MW |
| 208 | .6779 | | 9 | |
| 226 | .6792 | | 101 | |

TABLE IV continued

| hk·l | $\sin^2\theta$ (Å) Calculated $a_o = 5.093$, $c_o = 8.273$ | $\sin^2\theta$ Observed | Intensity Calculated | Intensity Observed |
|---|---|---|---|---|
| 405 | .7059 | .7061 | 148 | W |
| 316 | .7098 | -- | 32 | -- |
| 324 | .7194 | -- | 2 | -- |
| 109 | .7339 | -- | 22 | -- |
| 500 | .7638 | -- | 1 | -- |
| 218 | .7696 | .7710 | 118 | VW |
| 501 | .7725 | -- | 1 | -- |
| 325 | .7976 | | 50 | |
| 502 | .7985 | .7983 | 4 | VW |
| 406 | .8014 | | 81 | |
| 317 | .8226 | -- | 51 | -- |
| 330 | .8249 | | 81 | |
| 209 | .8255 | .8260 | 10 | VW |
| 308 | .8307 | | 85 | |
| 503 | .8419 | -- | 92 | -- |
| 420 | .8554 | -- | 36 | -- |
| 332 | .8596 | .8615 | 138 | W |
| 421 | .8641 | | 190 | |
| 0010 | .8682 | -- | 2 | -- |

TABLE IV continued

| hk·l | $\sin^2\theta$ (Å) Calculated $a_o = 5.093$, $c_o = 8.273$ | $\sin^2\theta$ (Å) Observed | Intensity Calculated | Intensity Observed |
|---|---|---|---|---|
| 422 | .8901 | -- | 19 | -- |
| 326 | .8931 | -- | 50 | -- |
| 1010 | .8988 | -- | 26 | -- |
| 504 | .9027 | -- | 16 | -- |
| 407 | .9142 | -- | 14 | -- |
| 219 | .9172 | -- | 77 | -- |
| 220 | .9223 | -- | 1 | -- |
| 423 | .9335 | -- | 4 | -- |
| 510 | .9471 | -- | 2 | -- |
| 318 | .9529 | .9512 | 261 | VW |
| 416 | .9542 | -- | 11 | -- |
| 511 | .9558 | -- | 4 | -- |
| 1110 | .9599 | -- | 6 | -- |
| 505 | .9809 | -- | 80 | -- |
| 512 | .9818 | -- | 23 | -- |
| 2010 | .9904 | -- | 606 | (too close to hole) |
| 424 | .9943 | -- | 13 | -- |

W = weak; M = medium; S = strong; V = very

TABLE V

Summary of the X-ray Data on Structure Types

| Alloy | Heat Treatment | Structure Type |
|---|---|---|
| $ZrCr_2$-$ZrFe_{1.6}Cr_{.4}$ | Arc melted, | Hexagonal C14 |
| $ZrFe_{1.8}Cr_{.2}$ | Arc melted | Cubic C15 |
| $ZrFe_2$ | Arc melted | Cubic C15 |
| $ZrCr_2$ | 1400°C 1 hour | Cubic C15 |
| $ZrFe_{.2}Cr_{1.8}$-$ZrFe_{1.6}Cr_{.4}$ | 1400°C 1 hour | Hexagonal C14 |
| $ZrFe_{1.8}Cr_{.2}$ | 1400°C 1 hour | Cubic C15 |
| $ZrFe_2$ | 1400°C 1 hour | Cubic C15 |
| $ZrCr_2$ | 1000°C 3 days | Cubic C15 |
| $ZrFe_{.2}Cr_{1.8}$ | 1000°C 3 days | Hexagonal C14 plus Cubic C15 |
| $ZrFe_{.4}Cr_{1.6}$-$ZrFe_{1.6}Cr_{.4}$ | 1000°C 3 days | Hexagonal C14 |
| $ZrFe_{1.8}Cr_{.2}$ | 1000°C 3 days | Cubic C15 |
| $ZrFe_2$ | 1000°C 3 days | Cubic C15 |
| $ZrCr_2$ | 890°C 30 days | Cubic C15 (partly transformed) |
| $ZrFe_{.2}Cr_{1.8}$ | 890°C 30 days | Hexagonal C14 plus Cubic C15 |
| $ZrFe_{.4}Cr_{1.6}$-$ZrFe_{1.6}Cr_{.4}$ | 890°C 30 days | Hexagonal C14 |
| $ZrFe_{1.8}Cr_{.2}$ | 890°C 30 days | Cubic C15 |
| $ZrFe_2$ | 890°C 30 days | Cubic C15 |

TABLE V continued

| Alloy | Heat Treatment | Structure Type |
|---|---|---|
| $ZrCr_2$ | 800°C 4 days | Hexagonal C14 |
| $ZrCr_2$, arc melted, as quenched | 890°C 15 days | C14 with Cubic C15 just beginning to appear |
| $ZrCr_2$, 1400°C 1 hour | 890°C 15 days | Cubic C15 |

TABLE VI

Summary of the X-ray Data on Lattice Constants

| Alloy | Heat Treatment | Lattice Constants in Å | Structure Type |
|---|---|---|---|
| $ZrFe_2$ | 890°C, 30 days | $a_o$ = 7.066 | Cubic C15 |
| $ZrFe_{1.8}Cr_{.2}$ | 890°C, 30 days | $a_o$ = 7.079 | Cubic C15 |
| $ZrFe_{1.6}Cr_{.4}$ | 890°C, 30 days | $a_o$ = 4.984<br>$c_o$ = 8.181 | Hexagonal C14 |
| $ZrFe_{1.4}Cr_{.6}$ | 890°C, 30 days | $a_o$ = 4.997<br>$c_o$ = 8.199 | Hexagonal C14 |
| $ZrFe_{1.2}Cr_{.8}$ | 890°C, 30 days | $a_o$ = 4.999<br>$c_o$ = 8.218 | Hexagonal C14 |
| ZrFeCr | 890°C, 30 days | $a_o$ = 5.008<br>$c_o$ = 8.236 | Hexagonal C14 |
| $ZrFe_{.8}Cr_{1.2}$ | 890°C, 30 days | $a_o$ = 5.024<br>$c_o$ = 8.254 | Hexagonal C14 |
| $ZrFe_{.6}Cr_{1.4}$ | 890°C, 30 days | $a_o$ = 5.037<br>$c_o$ = 8.277 | Hexagonal C14 |
| $ZrFe_{.4}Cr_{1.6}$ | 890°C, 30 days | $a_o$ = 5.051<br>$c_o$ = 8.297 | Hexagonal C14 |
| $ZrFe_{.2}Cr_{1.8}$ | 1400°C, 1 hour | $a_o$ = 5.065<br>$c_o$ = 8.303 | Hexagonal C14 |
| $ZrCr_2$ | 1400°C, 1 hour | $a_o$ = 7.193 | Cubic C15 |
| $ZrCr_2$ | Arc melt plus 800°C, 4 days | $a_o$ = 5.093<br>$c_o$ = 8.273 | Hexagonal C14 |

seemed to be only partly transformed and thus were not used for the calculations. For this purpose the samples at 1400°C were used to obtain the lattice constants of the cubic C15 $ZrCr_2$ and the hexagonal $ZrFe_{.2}Cr_{1.8}$. The latter was assumed to be a two phase alloy at 890°C. For the measurement of C14 $ZrCr_2$ the sample treated at 800°C for four days was used, homogeneity effects being not so essential here.

Figures 2 and 3 show graphically the results obtained. An explanation of these figures is perhaps necessary. In Figure 2 the hexagonal lattice constants are plotted against composition. As was mentioned before, it is possible to view a cubic structure hexagonally and that in so doing one does not alter the value of the $a_o$ parameter but only that of the $c_o$. Thus the values of $a_{hex}$ where the cubic structure is stable are those calculated from the cubic constant, $a_{cubic}$, by the relationship, $a_{hex} = a_{cubic}\sqrt{2}/2$. In this fashion, all data could be referred to the C14 structure in the hope that the behavior of these curves might lend some insight into the reasons why the hexagonal structure had transformed to cubic at another temperature or at a given composition limit. The $c_{hex}$ parameters were given only in the region where C14 was observed at one temperature or another and not beyond into the region where only the cubic structure was stable over the whole range of temperature. This reasoning applies similarly to Figure 3.

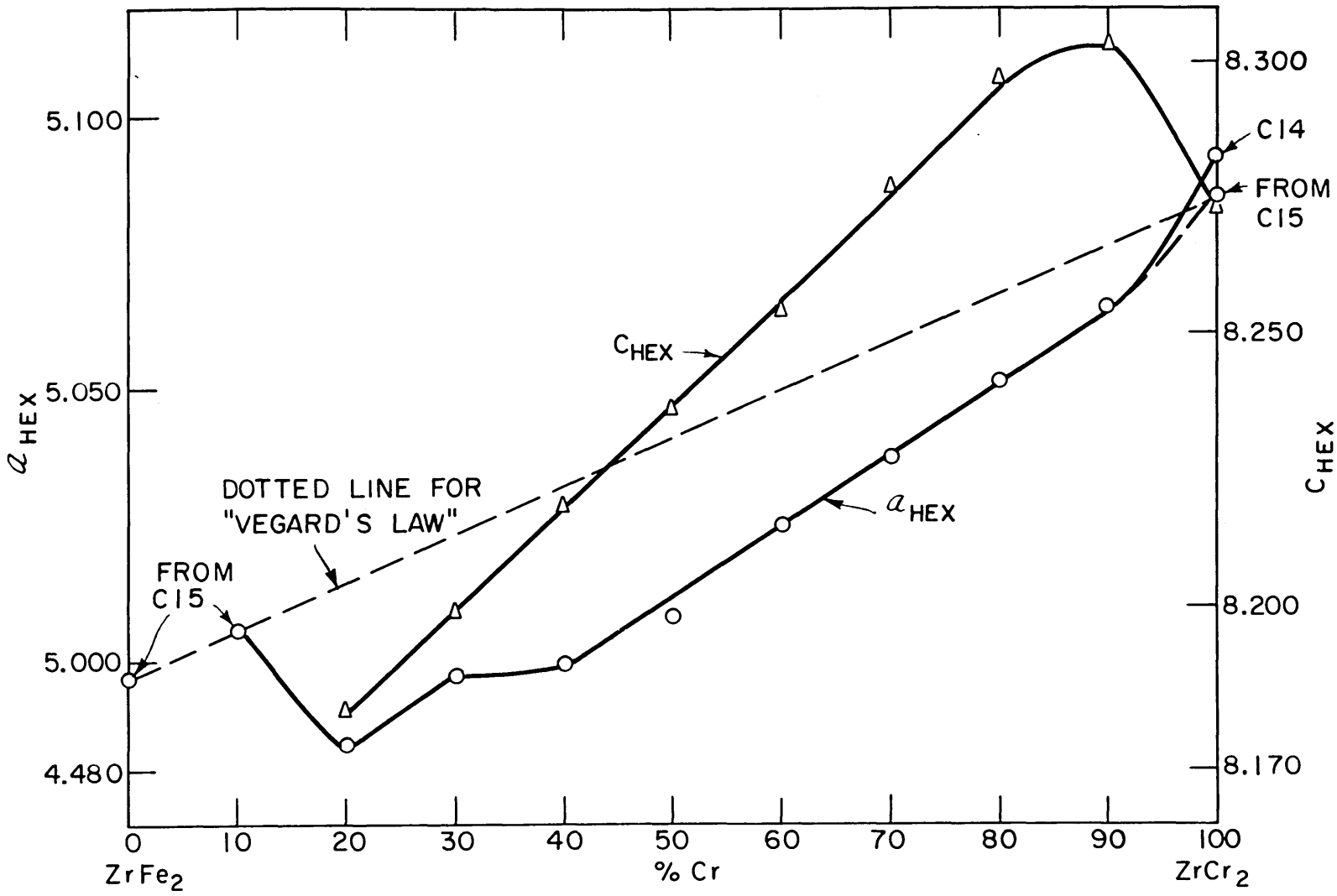


FIGURE 2. HEXAGONAL LATTICE CONSTANTS, $a_{HEX}$ AND $C_{HEX}$, VERSUS % Cr ACROSS THE PSEUDO BINARY SECTION, $ZrFe_2$ - $ZrCr_2$

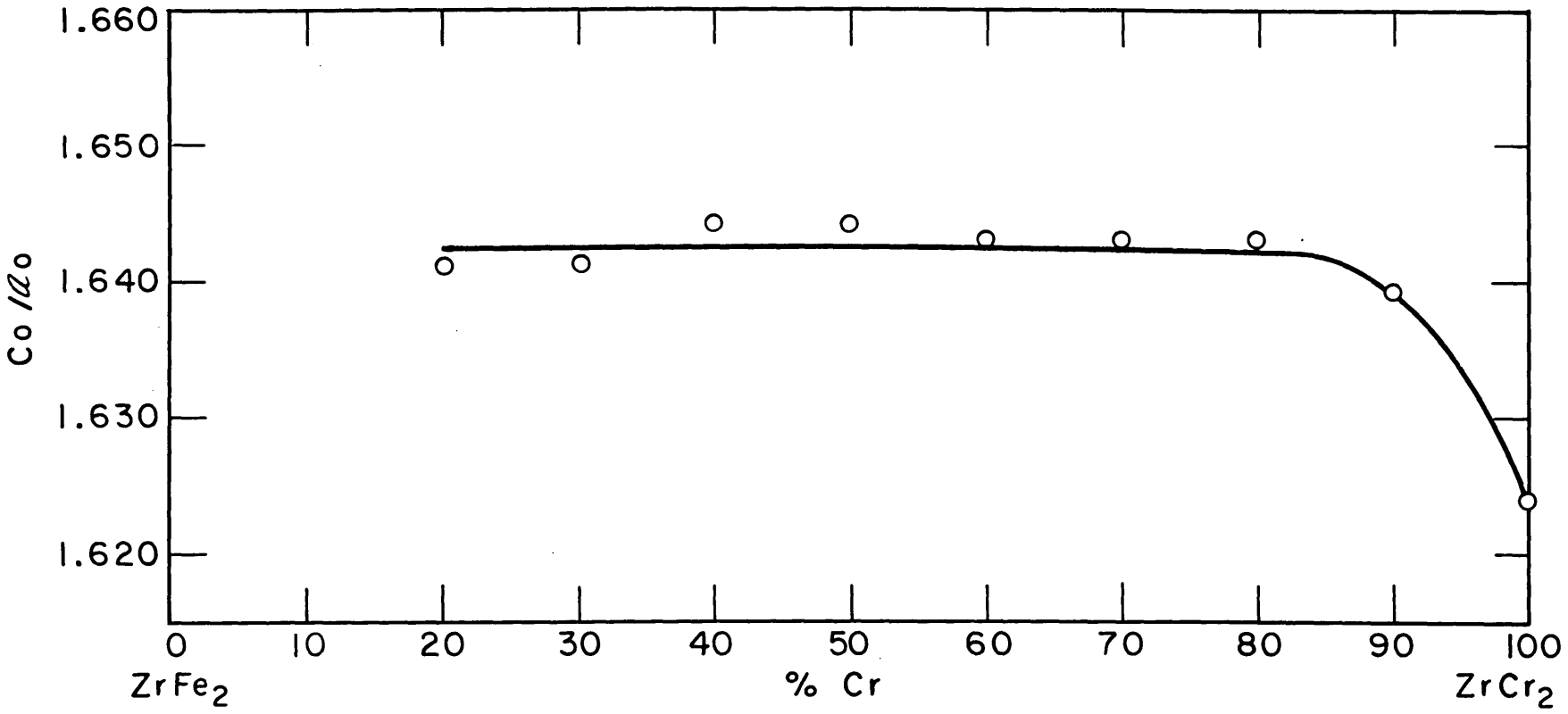


FIGURE 3. HEXAGONAL AXIAL RATIO Co/ao VERSUS % Cr FOR C14 STRUCTURE

# IV. Interpretation and Discussion

## A. Allotropy in $ZrCr_2$

The question of allotropy in $ZrCr_2$ discussed in the Introduction was considered of prime importance in this work. If regions of solubility are to be established across a ternary section it is necessary to know at what temperatures the structure data applies. The selected heat treatments given before and listed in Tables II and V help to illuminate the problem. It is felt that if $ZrCr_2$ has a high temperature structure of C15, as has been reported[12, 14], then this structure should appear as the structure of the arc melted button since $ZrCr_2$ melts congruently. As can be seen in Table V this is not the case. Again if the temperature of the transformation from low temperature C14 to high temperature C15 is between 900°C and 1000°C then an alloy treated at 890°C should show only C14 which did not prove to be the case. Rather the solubility limit of the C15 structure appeared to be greater at 890°C than at 1400°C. It may be argued that 890°C is too close to 900°C to be beyond the range of the transformation and that the partially transformed structure seen at this temperature was due to this fact. To clear the matter of any doubt, therefore, two samples -- one, C14 and the other, C15 transformed previously at 1400°C -- were

treated at 890°C as already described. The diffraction patterns showed that while the C14 structure had hardly begun to transform the C15 sample retained its cubic structure quite clearly.

The above results tend to confirm the argument of Jordan and Duwez[13] based on kinetic considerations. It is an entirely plausible argument when one considers that at 890°C it takes thirty days to partially transform C14 $ZrCr_2$ to C15, while at 1000°C it takes three days to complete the transformation and at 1400°C one hour is required. It is entirely justifiable to assume that at 600°C, 700°C, or even 800°C, the amount of time required to observe the stable C15 structure of $ZrCr_2$ is substantially longer than that given to any heat treatments so far reported in the literature[12, 13, 14]. The above evidence combined with Jordan's observation of the near melting point retransformation of C15 to C14 leads to the inevitable conclusion that, indeed the latter's reporting of C15 $ZrCr_2$ as the low temperature allotrope is correct.

## B. A Proposed Pseudo-Binary Section, $ZrFe_2$-$ZrCr_2$

In Figure 4 is presented a pseudo-binary phase diagram for the system here studied. Included are the results of the X-ray data upon which this diagram is based. Since the 1000°C

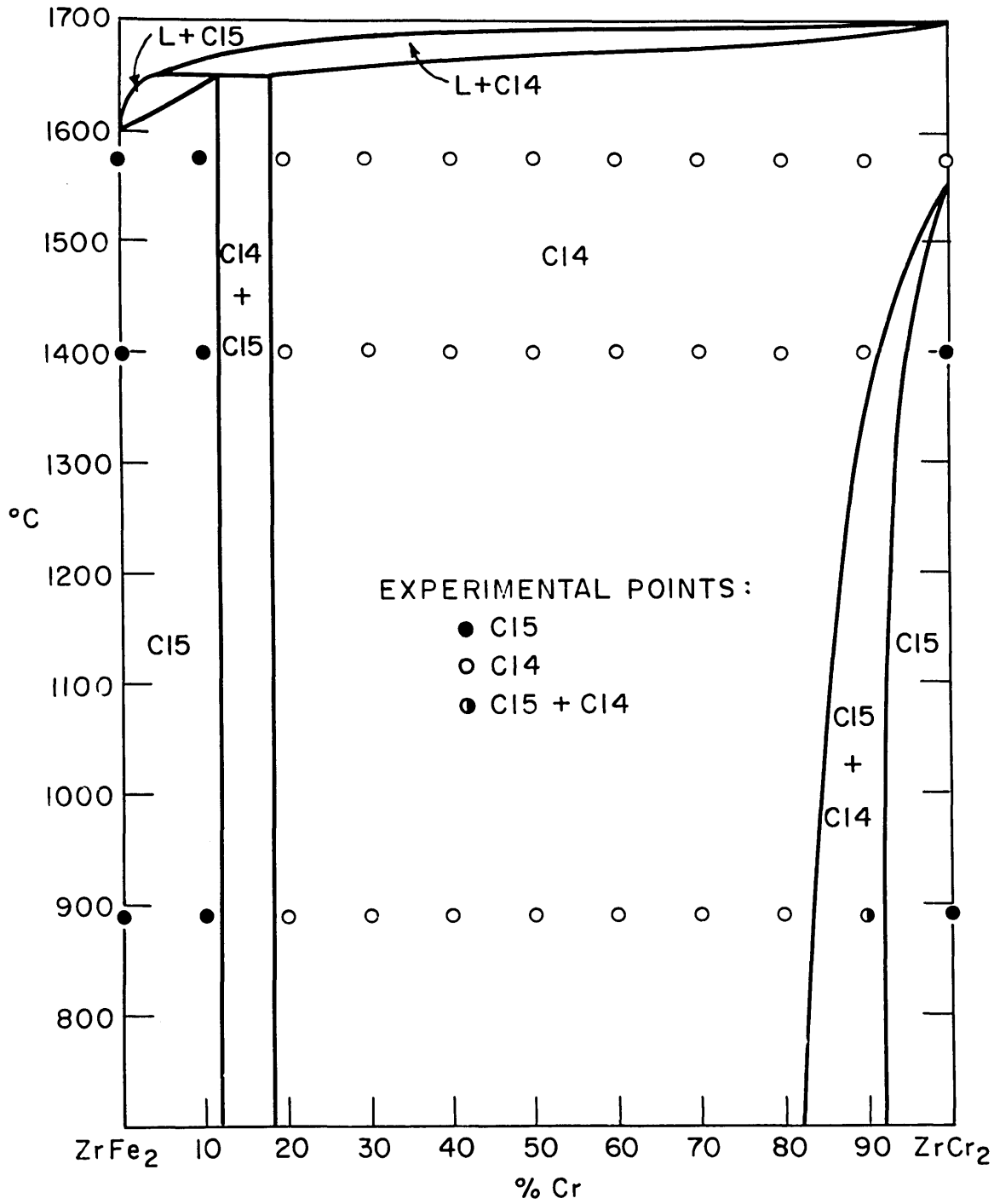


FIGURE 4. A PROPOSED PHASE DIAGRAM FOR THE PSEUDO-BINARY SECTION $ZrFe_2-ZrCr_2$

data essentially reconfirmed the 890°C data, they have been omitted for convenience. The high temperature data in which the solubility of C14 $ZrCr_2$ extends all the way to 80 percent iron is subject to some question because it represents measurements taken on the arc melted buttons. Coring problems hinder the assignment of accurate composition values for these alloys, and of course the temperatures at which they are listed are incorrect. Their actual temperatures cover a range in each case from where the first solid precipitates to where the last liquid freezes. This description is further distorted by the rapidity of the quench.

What can be said in defense of the presentation of the high temperature data in Figure 4 is that it is not in conflict with any of the other observations and that it does supply, in a general way, corroboration of the more accurate low temperature results. This could be said, actually, for the entire phase diagram. The temperature of the allotropic transformation in $ZrCr_2$ may be said only to occur in the region where it is set -- certainly above 1400°C and most assuredly below 1700°C. Again, referring to the work of Jordan and Duwez, one would expect this transformation temperature to lie fairly close to the melting point. The existence of the peritectic invariant on the iron rich end of the diagram and the gamma loop enclosing the low temperature modi-

fication of $ZrCr_2$, are based on some conjecture. The presentation is, however, the simplest phase diagram that could be constructed on the basis of the data.

C. A Proposed Ternary Isotherm at 800°C

The 800°C ternary section presented in Figure 5 is not really based upon the results herein presented, other than the fact that the system $ZrFe_2$-$ZrCr_2$ has been shown to be a true pseudo-binary. It is compiled on the basis of existing information concerning the Fe-Zr, Fe-Cr, and Zr-Cr binaries and is purposely taken below any invariant reactions in these systems to avoid complications resolvable only through more information about the ternary system itself.

D. Hexagonal Lattice Constants

Some additional interpretation should be given to Figure 2 where the values of the hexagonal lattice constants are plotted against percent Cr. In Figure 2 a theoretical line for Vegard's Law was drawn through those values of $a_{hex.}$ that were computed from cubic data; namely, for $ZrFe_2$, $ZrFe_{.8}Cr_{1.2}$ and $ZrCr_2$ (1400°C treatment). The basis for constructing such a line is that the Laves phase $AB_2$, may be considered, as before, as two separate lattices of A and B atoms. Were these two lattices to be truly independent, neglecting for the present any electronic interactions and

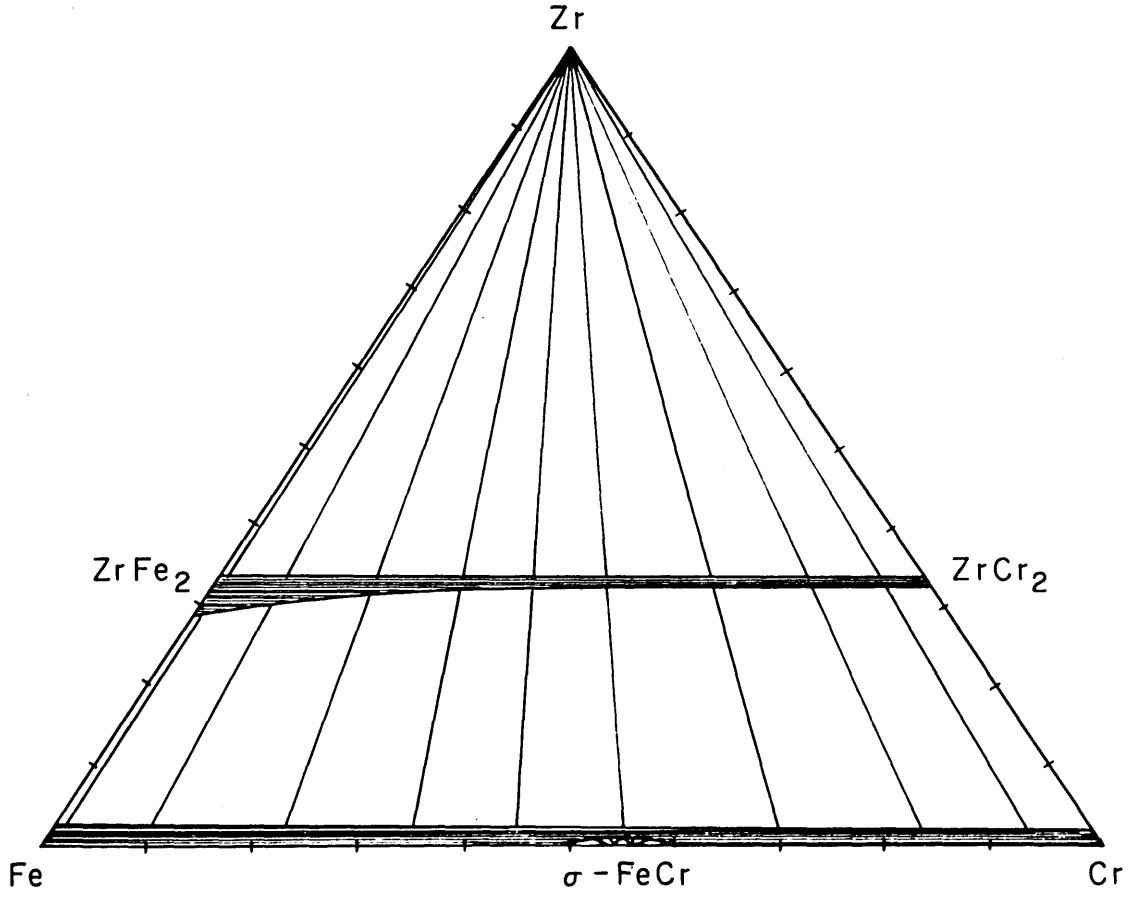


FIGURE 5. A PROPOSED 800°C ISOTHERM FOR THE TERNARY SYSTEM Zr-Fe-Zr

realizing that the stable low temperature phase is C15 at both ends of the pseudo binary section, Cr might be expected to substitute for Fe in the B lattice so as to produce a complete series of solid solutions. That this concept is not altogether improbable may be seen in the results of Elliott[8] where he and Rostoker report for the system $ZrFe_2$-$ZrCo_2$ a full range of miscibility.

In the range of solubility of the C15 structure in the present study it is interesting that near the iron rich end of the system the values of $a_{hex}$ do appear to follow some sort of linear behavior (when extrapolated as above). This behavior can be predicted by realizing that, for 12L coordination, the atom size of Cr is larger than that of Fe. It is then apparently peculiar that the $a_{hex}$ which is really a measure of the B-B distance, namely $a_{hex} = d_{B-B} \times 2$, should suddenly contract as it does at the composition $ZrFe_{.6}Cr_{1.4}$. This can be explained as a contraction of the B-B distance due to the accommodation of the lattice to the C14 structure for which the latter composition is the solubility limit. It seems that the transformation from C15 to C14 allows the interpenetrating lattice of B atoms, composed randomly of Fe and Cr atoms in the proportions designated, to undergo a relaxation.

The behavior of the A-A or Zr-Zr distance, reflected in

the $c_{hex}$ parameter and related to it by the expression ($c_{hex}$ = $8/3\ d_{A-A}$) can be interpreted as an attempt to accommodate the structure to the increasing B-B sizes. If one views the Laves phase as having an ideal ratio of $D_A/D_B$ = 1.225 where both A-A and B-B atoms touch, then an introduction of a large B atom, in its endeavor to fit into a prescribed space, must result at some point in a contraction of the B-B lattice and an expansion of the A-A lattice. The converse is also true. It is to be remembered that the above, pointed out by Berry and Raynor[9], applies only to deviations from the ideal packing. Furthermore this ideal packing should result in no atom distortions which again Berry and Raynor did not observe.

If the Laves phase is not ideal, which it hardly, if ever, is, then one might expect expansions to take place in the B-B distances with increasing B-B atom size until some structural accommodation is necessary whereupon the lattice would contract and a transformation would take place. Noticing the allotropy of the $ZrCr_2$, reflected by the two values of $a_{hex}$ in Figure 2, one now sees that a gross contraction of A-A distances ($c_{hex}$) is necessary to stabilize the C14 modification. This is observed more easily in Figure 3 where only values for the C14 axial ratios are plotted. It is in this area of proposed instability that the low temperature $ZrCr_2$ prefers the cubic stacking to relieve the compression

of A-A atoms. It is realized that the above arguments merely are a way of essentially restating the fact that a transformation does take place and is accompanied by structural relaxations.

E. Bond Distortions

Berry and Raynor[9] introduced a systematic way of plotting bond distortions in an attempt to make some correlation with the theoretical atom size ratios, $D_A/D_B$. In Figure 6 are plotted these distortions as percentages, S, of the size in the pure metal (corrected to 12L) for each specie. The values of S are obtained from the present data in the following manner:

$$S_{AA}(\%) = \frac{d_{AA} - D_A}{D_A} \quad (100) \qquad (2)$$

$$S_{BB}(\%) = \frac{d_{BB} - D_B}{D_B} \quad (100) \qquad (3)$$

where $d_{AA}$ and $d_{BB}$ are the A-A and B-B distances obtained from the values of $c_{hex}$ and $a_{hex}$ as shown in the last section and given in Table VIII and $D_A$ and $D_B$ are the atomic diameters in the pure metal related to 12L coordination, obtained from Elliott[14] and given in Table VII. The absolute values of S are rather misleading because they show that in all cases

TABLE VII

Values of $D_A$ and $D_B$, Atomic Diameters in the Pure Metal Corrected to Twelve Fold Coordination, and the Ratios $D_A/D_B$

| Alloy | $D_A$ (Zr), Å | $D_B$ (Fe,Cr) Å | $D_A/D_B$ |
|---|---|---|---|
| $ZrFe_2$ | 3.201 | 2.525 | 1.268 |
| $ZrFe_{1.8}Cr_{.2}$ | 3.201 | 2.430 | 1.265 |
| $ZrFe_{1.6}Cr_{.4}$ | 3.201 | 2.535 | 1.263 |
| $ZrFe_{1.4}Cr_{.6}$ | 3.201 | 2.540 | 1.260 |
| $ZrFe_{1.2}Cr_{.8}$ | 3.201 | 2.545 | 1.258 |
| ZrFeCr | 3.201 | 2.550 | 1.255 |
| $ZrFe_{.8}Cr_{1.2}$ | 3.201 | 2.555 | 1.253 |
| $ZrFe_{.6}Cr_{1.4}$ | 3.201 | 2.560 | 1.250 |
| $ZrFe_{.4}Cr_{1.6}$ | 3.201 | 2.565 | 1.248 |
| $ZrFe_{.2}Cr_{1.8}$ | 3.201 | 2.570 | 1.246 |
| $ZrCr_2$ | 3.201 | 2.575 | 1.243 |

TABLE VIII

Values of $d_{AA}$ and $d_{BB}$, Distances in the Alloys as Calculated from $a_{hex}$ and $c_{hex}$, and the Ratios $d_{AA}/d_{BB}$

| Alloy | Structure Type | $d_{AA}$ | $d_{BB}$ | $d_{AA}/d_{BB}$ |
|---|---|---|---|---|
| $ZrFe_2$ | C15 | 3.060 | 2.498 | 1.225 |
| $ZrFe_{1.8}Cr_{.2}$ | C15 | 3.065 | 2.502 | 1.225 |
| $ZrFe_{1.6}Cr_{.4}$ | C14 | 3.068 | 2.492 | 1.231 |
| $ZrFe_{1.4}Cr_{.6}$ | C14 | 3.075 | 2.499 | 1.230 |
| $ZrFe_{1.2}Cr_{.8}$ | C14 | 3.082 | 2.500 | 1.233 |
| ZrFeCr | C14 | 3.089 | 2.504 | 1.234 |
| $ZrFe_{.8}Cr_{1.2}$ | C14 | 3.095 | 2.512 | 1.232 |
| $ZrFe_{.6}Cr_{1.4}$ | C14 | 3.104 | 2.519 | 1.232 |
| $ZrFe_{.4}Cr_{1.6}$ | C14 | 3.111 | 2.526 | 1.232 |
| $ZrFe_{.2}Cr_{1.8}$ | C14 | 3.114 | 2.533 | 1.229 |
| $ZrCr_2$ | C14 | 3.102 | 2.547 | 1.218 |
| $ZrCr_2$ | C15 | 3.114 | 2.543 | 1.225 |

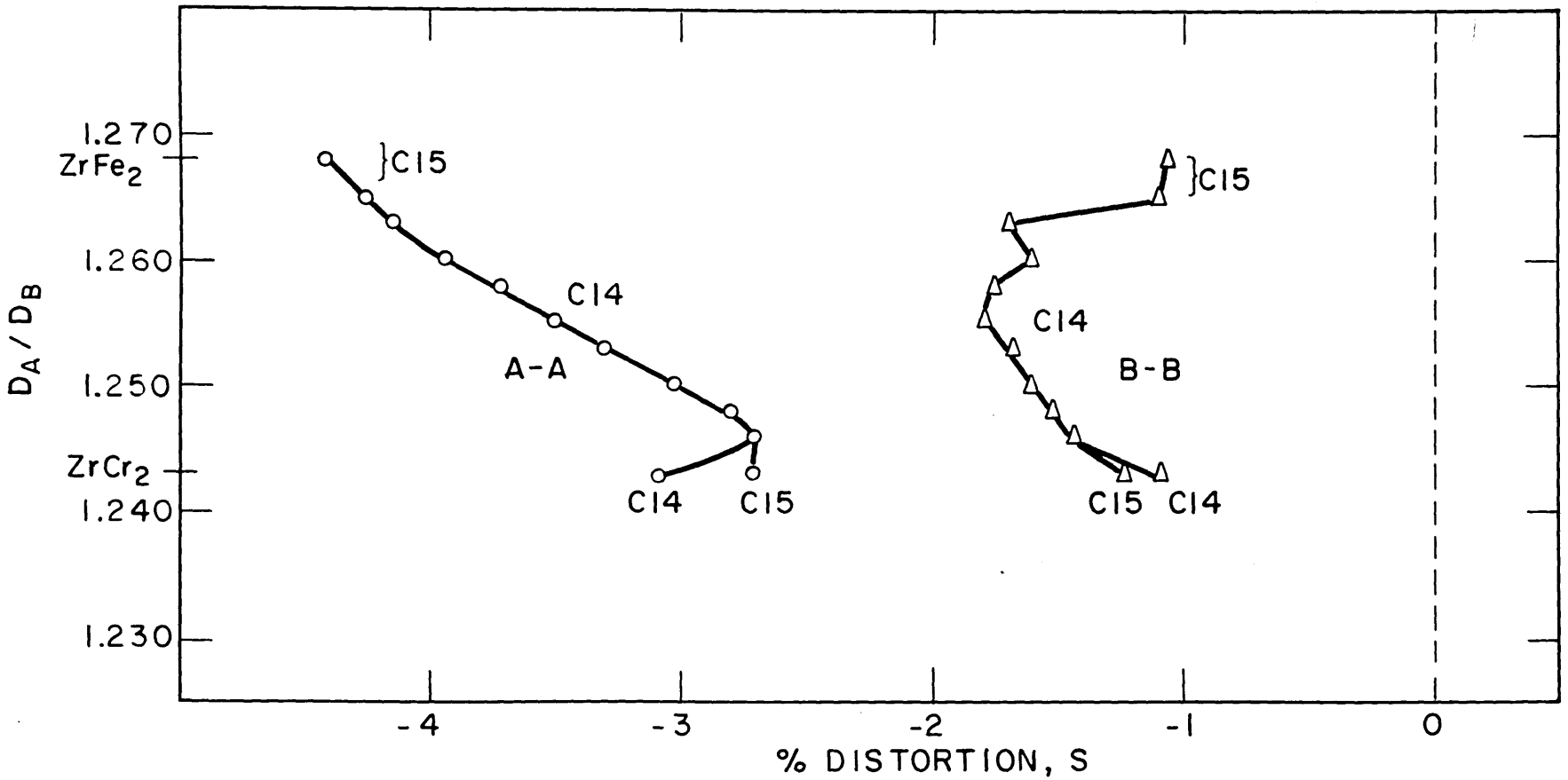


FIGURE 6. RATIO OF CALCULATED ATOM SIZES, $D_A/D_B$ (CORRECTED TO 12L), VERSUS MEASURED % DISTORTION, S

in the system $ZrFe_2$-$ZrCr_2$ contractions are observed. Thus only changes relative to the binary components are meaningful. Atom sizes in general are such a fiction that it is difficult really to talk of them. Laves[4] pointed out this difficulty but rationalized it in terms of gross behavior and the general applicability of the size ratio to the prediction of Laves phase occurence. He indicated that as the size ratio $D_A/D_B$ increased or decreased from 1.225, the corresponding Laves phases showed A-A and B-B distortions in an amount sufficient to retain the phase. Taken over a large number of compounds Laves' data corroborates this argument. Similarly the data of Elliott[14] illustrates the above behavior over a number of binary Laves phases taken with Zr as the A element. Figure 7 is a reproduction from Elliott.

Berry and Raynor plot similar data for Zr but connect only those binaries where the B element is of the same subgroup, thus forming sets of intersecting A-A and B-B distortions plotted against $D_A/D_B$. These sets are explained, for the transition elements, on the basis of strong electronic interactions. Furthermore their choice of $D_A$ and $D_B$ is the uncorrected size in the pure metal. One thus sees how predicted behavior depends upon a fairly arbitrary choice of atom size, especially if detailed behavior is in question. Figure 6 of the present work may be interpreted in view of the portions of Elliott's plot in Figure 7 which lie on the curves between

Fe and Cr. One questions the real meaning of Figure 7 preferring instead accurate data on the system $ZrCr_2$-$ZrMo_2$ or $ZrCr_2$-$ZrW_2$. Would the curves of Figure 7 be reproduced if distortions in these binaries were examined? It is a difficult question to answer and one which may even be irrelevant in that the behavior of such a pseudo-binary system is very much dependent upon interactions peculiar to that system. Thus Figure 6 illustrates that for the system $ZrFe_2$-$ZrCr_2$, the transformation near the iron rich end is a result really of B-B distortions, the A-A distances not reflecting very much of a change. At the Cr rich end, $ZrCr_2$, it seems that the Zr-Zr distance is the controlling factor in not being able to sustain the severe contraction that the C14 stacking requires.

Another interpretation of the data that proves interesting is seen in Table VIII. The atom "sizes" $d_{AA}$ and $d_{BB}$ are listed together with an observed size ratio of $d_{AA}/d_{BB}$ for each alloy. The atoms of the C15 cubic structure are seen to readjust themselves to accommodate to the theoretical size ratio, 1.225 while the atoms of the C14 structure adjust to a slightly greater ratio except perhaps for $ZrFe_{.2}Cr_{1.8}$ which has been shown before to tend to transform to C15 as the temperature is lowered. It is not known if this behavior has been observed in other systems as the data is not available.

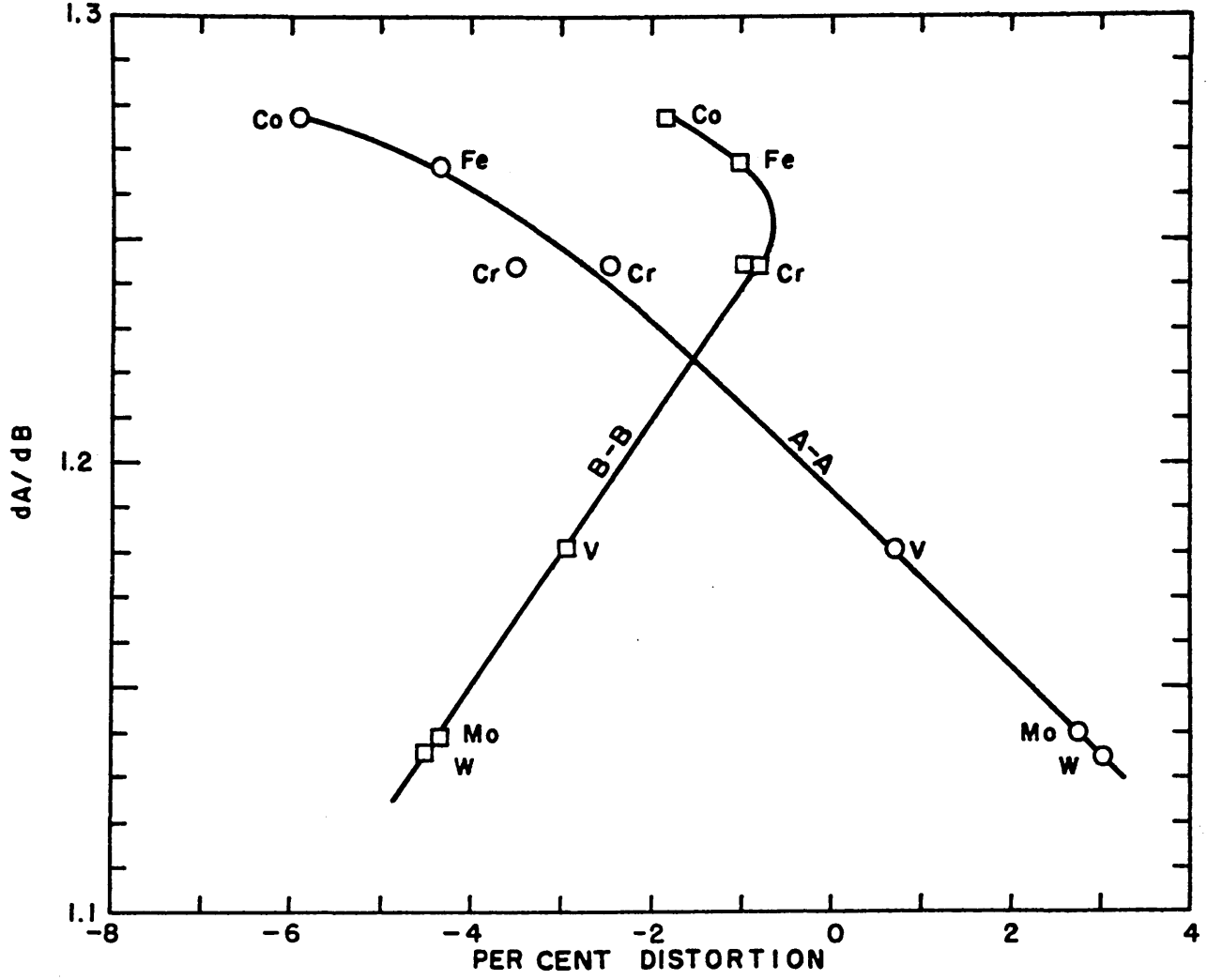


FIG. 7 - DISTORTION IN A-A AND B-B BONDS FOR $AB_2$ LAVES PHASES AS A FUNCTION OF ATOMIC DIAMETER RATIO dA/dB. A = ZIRCONIUM. After Elliott[14].

F. Electronic Considerations

The electronic interpretation of Laves phase stability, presented by Elliott and Rostoker[8] for transition metals is quite interesting but subject to some argument. Those authors based their calculation of transition element valencies upon the ranges that Laves and Witte[7] and Witte and Klee[6] gave for electron concentration within which the separate Laves phases, C15, C36 and C14, were stable. Laves' and Witte's observations were based upon a simple electron/atom model as given by the standard valencies in the periodic table for non-transition elements. The Witte and Klee values were obtained from magnetic measurements and their relation to Brillouin zones. There is no reason to assume that the electron concentrations of the Brillouin zones of the Laves phases of transition elements is the same as that of the ordinary metals of the non-transition groups.

While Elliott's work represents perhaps the most extensive application of available theory, it is not felt here that electron concentration limits as obtained from work on other systems can be the sole cause of the instability of the particular structures in question. Most of Elliott's calculations were based upon an assumed valency of Zr based upon the supposed near tetra-valence of Ti. However, small changes in this Zr valence affect the valencies of the other

metals measured. Furthermore, the present work shows the stable low temperature structure of $ZrCr_2$ to be C15 in disagreement with Elliott. This fact would alter greatly the latter's value of the electron/atom concentration or valency of Zr and thus the valencies of the other metals. As indicated before, there are some fairly large size changes accompanying the C14 to C15 transformation. These size effects surely vary with the system under study and make the exact assignment of the same electron/atom values to solubility limits in all systems rather tenuous.

The reasoning above is not meant to imply that electron concentrations are negligible or size ratios paramount in the stability of these phases. It is merely meant to imply that caution must be taken in the abrupt delineation of such obviously coupled effects.

## G. Other Considerations

What can be said with assurance is that the several component elements of the free energy, F, for a particular phase must combine in such a way as to minimize this term. These elements may be broken down roughly into atomic and electronic contributions to the bonding energy or heat of formation, composed of both configurational (positional) and vibrational terms. Since these are related by the equation,

F = E -TS, a temperature effect will of course be observed and all of these factors will also depend upon composition. The free energy behavior of ternary systems is quite complex and no attempt at a thermodynamic analysis will be made. It should suffice to say that such an analysis might prove useful were it possible to include all of the relevant terms.

Another phenomenon that may well be occurring is the selective ordering of either Fe or Cr atoms as they are substituted for their opposite member. The possibility of such long range order was suggested in part by Brook, Williams and Smith in their observations on the system $UFe_2$-$UNi_2$[20]. Long range order would be suspected mostly in systems where the atom sizes of the two types of B atoms do not differ by very much. In many cases such a closeness in size is due to proximity in the periodic table of the elements as for Fe-Ni or Fe-Cr. When the atomic numbers of the two elements are so similar, the scattering factors are too close to each other to allow superlattice lines of an ordered structure ordinarily to be detected. The X-ray problem is not an impossible one as shown by Skolnick et. al.[21] in their work on ferrites. If ordering exists, other measurements such as heat capacity should provide helpful information. That ordering might be expected is not unlikely if one remembers that the three modifications of Laves phases differ essentially only in stacking sequence.

## V. Conclusions

From the present study of structural relationships in the pseudo-binary system $ZrFe_2$-$ZrCr_2$ certain conclusions can be drawn.

1. The allotropy of $ZrCr_2$ has been established with the hexagonal C14 type as the high temperature modification and the cubic C15 type as the low temperature structure.

2. A proposed pseudo-binary phase diagram has been constructed on the basis of X-ray data on the as-quenched arc melted buttons and on heat treatments of these buttons at 1400°C, 1000°C, and 890°C. This phase diagram contains a peritectic invariant at the iron rich end to account for the transformation of the iron rich cubic C15 structure to the hexagonal C14 type at larger Cr percentage. After a narrow two phase region, this C14 type extends completely across the diagram at the very high temperatures and up to the cubic $ZrCr_2$ at lower temperatures. It seems that the solubility of cubic $ZrCr_2$ increases as the temperature decreases below the allotropic transformation point. To account for the low temperature C15 $ZrCr_2$, a gamma loop enclosing this phase has been included.

3. Size effects have been studied and it has been shown that at the iron rich end the transformation from cubic

to hexagonal is accompanied by structural relaxations manifested by a sharp decrease in the B-B atom distances, where the ternary phase is represented by $AB_2$ with Zr as the A atom and the combination (Fe,Cr) as the B atom. At the Cr rich end the retransformation from hexagonal to cubic is accompanied mainly by relaxations in the A-A or Zr-Zr distortions.

4. It also appears that the cubic structure accommodates itself to an observed radius ratio of $d_{AA}/d_{BB} = 1.225$ which is the ideal ratio for Laves phases. The hexagonal structure seems to exhibit an observed ratio slightly higher than this latter value in all cases.

# BIBLIOGRAPHY


1. J. B. Friauf, J. Am. Chem. Soc., 49 (1927), 3107-3114.

2. J. B. Friauf, Phys. Rev., 29 (1927), 35-40.

3. F. Laves and H. Witte, Metallwirtschaft, 14 (1935), 645-649.

4. F. Laves, Theory of Alloy Phases, 1956, 124-198: Cleveland, Ohio (Am. Soc. for Metals).

5. T. B. Massalski, Theory of Alloy Phases, 1956, 63-123: Cleveland, Ohio (Am. Soc. for Metals).

6. H. Klee and H. Witte, Zeit. fur Phys. Chemie, 202 (1954), 352.

7. F. Laves and H. Witte, Metallwirtschaft, 15 (1936), 840.

8. R. P. Elliott and W. Rostoker, Trans. of the ASM, 50 (1958), 617-632.

9. R. L. Berry and G. V. Raynor, Acta Cryst., 6 (1953), 178-186.

10. H. J. Wallbaum, Naturwissenschaften, 30 (1942), 149.

11. Zirconium Alloy Investigations, U. S. Bureau Mines, Tech. Prog. Rept. 4, 1 Sept. - 1 Nov., 1950.

12. W. Rostoker, J. Metals, 5 (1953), 304.

13. C. B. Jordan and P. Duwez, JPL Prog. Rept. No. 20-196, June 16, 1953.

14. R. P. Elliott, Armour Res. Foundation, Tech. Repts. Nos. 1 and 2 to Air Research and Development Command, Aug. 23, 1954 and Dec. 20, 1954.

15. H. J. Wallbaum, Arch. Eisenhuttenw., 14 (1941), 521-526.

16. N. Peterson, M. S. Thesis, M. I. T., Feb. 1959.

17. J. B. Nelson and D. P. Riley, Proc. Phys. Soc., 57 (1945), 645.

18. C. J. Smithells, Metals Reference Book, 1955, 172, New York, Interscience Publishers Inc.

19. B. D. Cullity, Elements of X-ray Diffraction, 1956, Reading, Mass., Addison Wesley Publishing Co., Inc.

20. G. B. Brook, G. I. Williams and (Mrs.) E. M. Smith, J. Inst. of Metals, 83 (1954), 271-276.

21. L. P. Skolnick, S. Kondo and L. R. Levine, J. App. Phys., 29 (1958), 198-203.

# APPENDIX I

## A Sample Calculation of the Phase Factor, A, Used in the Determination of the Structure Factor, F, for the C14 Structure

$$F = \sum_n f_n \left[\cos\ 2\pi (hx_n + ky_n + lz_n) + \right.$$

$$\left. + \ i \sin 2\pi (hx_n + ky_n + lz_n)\right].$$

$$F = \sum_n f_n A_n + \sum_n f_n B_n$$

$$|F|^2 = \left[\sum_n f_n A_n\right]^2 \qquad \text{where } B = 0 \text{ for space group } D_{6h}^4 - P6_3/mmc$$

For $ZrCr_2$, C14 structure:

2 Cr in 2(a) : 000, 001/2

6 Cr in 6(h) : $\pm$(x, x, 1/4; $2\bar{x}$, $\bar{x}$, 1/4; x, $\bar{x}$, 1/4), x = -1/6

4 Zr in 4(f) : $\pm$(1/3, 2/3, z; 2/3, 1/3, 1/2 + z), z = 1/16

$$A_{Cr(2a)} = 2 \cos 2\pi (l/4) \left[\cos \pi (-l/2)\right]$$

$$A_{Cr(6h)} = 2 \cos 2\pi (l/2) \left\{ \cos \pi (-h-k)(15/6) \left[\cos\ \pi\ (k-h)\,5/6 - l/2\right] + \right.$$
$$+ \cos \pi\, h\ (15/6)\ \cos \pi \left[(2k+h)\ (-5/6)\ - l/2\right] +$$
$$\left. + \cos \pi\, k\ (15/6)\ \cos \pi \left[(2h+k)\ (5/6)\ - l/2\right]\right\}.$$

$$A_{Zr(4f)} = 4/3 \cos 2\pi(5l/16) \left\{\cos\pi(-h-k)\ \cos\pi\left[(k-h)\,(1/3)\ - l/2\right] + \right.$$
$$+ \cos \pi\, h\ \cos \pi \left[(2k+h)\,(-1/3)\ - l/2\right] +$$
$$\left. + \cos \pi\, k\ \cos \pi \left[(2h+k)\ (1/3)\ - l/2\right]\right\}.$$

For the reflection 322 :

| $A_{Cr(2a)}$ | $A_{Cr(6h)}$ | $A_{Zr(4f)}$ |
|---|---|---|
| 2.000 | -1.000 | -1.414 |

$$F = f_{Cr}\left[A_{Cr(2a)} + A_{Cr(6h)}\right] + f_{Zr}\left[A_{Zr(4f)}\right]$$

$$F = f_{Cr} - 1.414\, f_{Zr}$$

# APPENDIX II

## Calculation of the Hexagonal Lattice Constants $a_o$ and $c_o$ of $ZrCr_2$ by the Least Squares Technique

Equation for hexagonal lattice constants:

$$\sin^2\theta - A_o\alpha - C_o\gamma = \epsilon \qquad \text{where } \alpha = h^2 + hk + k^2$$

$$\gamma = l^2$$

$$A_o = \lambda^2/3a_o^2$$

$$C_o = \lambda^2/4c_o^2$$

$\epsilon$ = error or drift

Normal equations for above:

$$\sum \alpha^2 A_o + \sum \alpha\gamma C_o = \sum \alpha \sin^2\theta$$

$$\sum \alpha\gamma A_o + \sum \gamma^2 C_o = \sum \gamma \sin^2\theta$$

| hkl | $\sin^2\theta$ | $\alpha$ | $\gamma$ |
|---|---|---|---|
| 323 | .6590 | 19 | 9 |
| 405 | .7061 | 16 | 25 |
| 218 | .7710 | 7 | 64 |
| 318 | .9512 | 13 | 64 |

| | |
|---|---|
| $\sum \alpha^2 =$ | 835 |
| $\sum \gamma^2 =$ | 8898 |
| $\sum \alpha\gamma =$ | 1851 |
| $\sum \alpha \sin^2\theta =$ | 41.5812 |
| $\sum \gamma \sin^2\theta =$ | 133.8043 |

1) $835\ A_o + 1851\ C_o = 41.5812$

2) $1851 A_o + 8898\ C_o = 133.8043$

$$A_o = .0305508 = \lambda^2/3a_o^2$$

$$C_o = .0086824 = \lambda^2/4c_o^2$$

$CuK_\alpha$ : $\lambda = 1.54178 \mathring{A}$

$$a_o = 5.093$$

$$c_o = 8.273$$

$$c_o/a_o = 1.624$$